Analysis of Ion Motion and Diffusion Confinement in Inverted Drift Tubes and Trapped Ion Mobility Spectrometry Devices.

Carlos Larriba-Andaluz[1*], Xi Chen[1,2], Minal Nahin[1], Tianyang Wu[1], Nobuhiko Fukushima[3]

[1]IUPUI, Department of Mechanical Engineering, 723 W Michigan st., Indianapolis, IN, 46202, USA. [2]Purdue University, West Lafayette, IN, 47907, USA.[3]Kanomax Japan Inc., Shimizu, Suita-shi, Osaka, 565-0805, Japan

ABSTRACT: Ion motion in Trapped Ion Mobility Spectrometers (*TIMS*) and Inverted Drift Tubes (*IDT*) has been investigated. The 2D axi-symmetric analytical solution to the Nernst-Planck equation for constant gas flows and opposed linearly increasing fields is presented for the first time and is used to study the dynamics of ion distributions in the ramp region. It is shown that axial diffusion confinement is possible and that broad packets of ions injected initially into the system can be contracted. This comes at the expense of the generation of a residual radial field that pushes the ions outwards. This residual electric field is of significant importance as it hampers sensitivity and resolution when parabolic velocity profiles form. When RF is employed at low pressures, this radial field affects the stability of ions inside the mobility cell. Trajectories and frequencies for stable motion are determined through the study of Mathieu's equation. Finally, effective resolutions for the ramp and plateau regions of the *TIMS* instrument are provided. While resolution depends on the inverse of the square root of mobility, when proper parameters are used, resolutions in the thousands can be achieved theoretically for modest distances and large mobilities.

INTRODUCTION

Ion Mobility Spectrometry (IMS) involves a compendium of techniques with the purpose of segregating small charged entities- molecules or nanoparticles- by means of an electrical field in the presence of a buffer gas. IMS relies strongly on the ability of ions to quickly reach an equilibrium drift velocity, v_{drift}, akin to a settling or terminal velocity. Moreover, under small ion velocities, the electrical/ion mobility is directly related to the product of the drift velocity and the electric field through a simple equation: $KE \sim v_d$. Ion mobility can then be related to ion size, charge and gas properties through the use of either the Stokes-Millikan[1,2] semi-empirical law or the more theoretical Mason-Schamp equation[3]:

$$K = \frac{3}{16}\frac{q}{N}\left(\frac{1}{m}+\frac{1}{M}\right)^{1/2}\sqrt{\frac{2\pi}{k_b T}}\frac{1}{\Omega} \qquad (1)$$

Here, N is the gas number density, T is the temperature, q is the ion's charge, k_b is the Boltzmann's constant, m and M are the mass of the gas and ion respectively, and Ω is the ion's Collision Cross Section (*CCS*)[4]. Owing to this physical simple and controllable relation between electrical field and gas, IMS has been gaining momentum in both Aerosol Science and Analytical Chemistry fields, becoming one of the most prominent separation techniques. As such, a myriad of IMS systems are emerging. Among such systems one can name the most conventional ones, Drift Tube (*DTIMS*)[5] and Differential Mobility Analyzer (*DMA*)[6], which have been available since the 1970s. Recently, many techniques and systems have appeared, including the Transversal Modulated Wave (*T-Wave*)[7], Field Asymmetric Ion Mobility Spectrometry (*FAIMS*)[8], Overtone Mobility Spectrometer (*OMS*)[9], Differential Mobility Spectrometer (*DMS*)[10], Radial Opposed Migration of Ion and Aerosol Classifier (*ROMIAC*)[11], Fast Integrated Mobility Spectrometer (*FIMS*)[12], Structure for Lossless Ion Manipulation (*SLIM*)[13], Diffusion Differential Analyzer (*DDA*)[14], Trapped Ion Mobility (*TIMS*)[15,16] and Inverted Drift Tube (*IDT*)[17].

Arguably, one of the most significant problems in IMS systems, common to all the aforementioned systems, is ion diffusion. The "random" movement of ions in the gas phase leads to lower resolution, transmission, and, ultimately, overall sensitivity. As such, it is of particular importance to constrain, regulate or overcome diffusion to obtain optimal separation results. For the purpose of this study, and given that most IMS instruments have a well-defined axis of revolution, diffusion can be divided into a) Radial diffusion, perpendicular to the axis of revolution and cause of lowering overall transmission and b) Axial diffusion, parallel to the axis of revolution and which in general lowers overall resolution. Radial diffusion has been partially counteracted at low gas pressures through the use of radio-frequency (RF) confining voltages[18]. However, the high frequency and voltages required to contain ions at high pressures precludes the use of RF in atmospheric pressure devices. Trying to overcome Axial diffusion, some systems resort to increasing the length of the characterization region, e.g. *T-wave* and *DTIMS*. It can be shown theoretically that, given Einstein-Smoluchowski's[19] relation under ideal conditions, two ions of different mobilities under a constant field will separate if given sufficient length (or time). Noteworthy is the recent accomplishment separating isomers using *SLIM* systems[20].

It is however the *TIMS* and *IDT* systems that are the main focus of this manuscript for their unique ability to constrain Axial diffusion. The two systems have in common a separation region where a flow of gas with velocity $\vec{v}_{gas}$

This is the author's manuscript of the article published in final edited form as:
Larriba-Andaluz, C., Chen, X., Nahin, M., Wu, T., & Fukushima, N. (2018). Analysis of Ion Motion and Diffusion Confinement in Inverted Drift Tubes and Trapped Ion Mobility Spectrometry Devices. Analytical Chemistry. https://doi.org/10.1021/acs.analchem.8b03930

carries the ion forward while a linearly increasing electric field of the type $\vec{E}_z = -Az\vec{k}$ opposes the movement of the ions –a technique previously developed by Zeleny[21] in gases and also proven in liquid phase experiments[22]. Here, A is the slope of the field, z is the position in the axial direction and $\vec{k}$ is the unit vector in that direction. The ion's movement in the axial direction is thus characterized by the competition between gas and drift velocity so that the ion's velocity is given by $\vec{v}_{z_{ion}} = \vec{v}_{gas} - \vec{v}_{drift}$. In the *TIMS* instrument, ions can be stopped/trapped, $\vec{v}_{z_{ion}} = 0$[23], and are kept from colliding with the electrodes through the use of RF fields. The portion of the tube dedicated to stopping the ions, is known as the trapping (ramp or rising edge) region. Once trapped, the electric field is lowered, and the ions are "eluted" through a plateau region -constant electric field- and eventually transmitted to a Mass Spectrometer. While the trapping typically takes 10s of ms, the elution happens in less than a ms. Diffusion confinement is therefore the main working principle in *TIMS*. A schematic of the process is shown in Figure 1. The *IDT*, in contrast, works at atmospheric pressure and, as such, cannot make use of RF fields to constrain the ions radially. Under these circumstances, the ion must be kept in constant movement, $\vec{v}_{z_{ion}} \neq 0$, and a parameter labeled the separation ratio, $\Lambda = v_{drift}/v_{gas} \leq 1$, is used to specify the movement[17]. This parameter plays a key role in the ability of the *IDT* to resolve different ions.

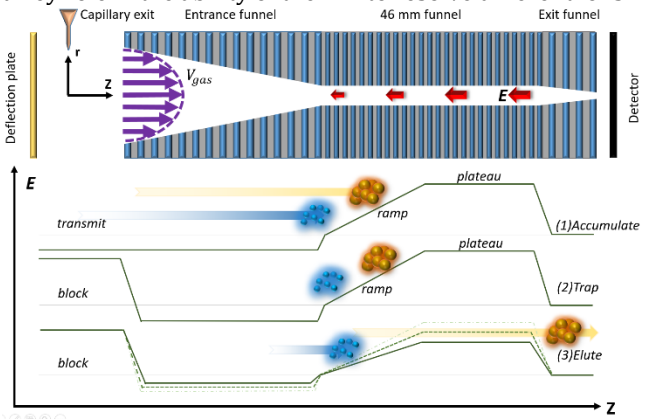

Figure 1. Sketch of *TIMS* setup.

In either system, it is the combined effect of both velocities, drift and gas, that controls Axial diffusion. However, the complexity of the electro-fluid-dynamic interaction makes its analytical interpretation and understanding quite difficult. Prior to this manuscript, there has been a few attempts at solving the equations of motion partially. Michelmann, Silveira and colleagues described ion motion, focusing on the equilibrium position at the end of the ramp, on the elution portion of the plateau and on the gas flow characterization[23,24]. They did in fact describe a confining electric potential so that "a deviation of the ions from the equilibrium position will therefore result in a net restoring force equal to the ions' charge multiplied by the difference in the electric field strength between the equilibrium position and the deviant position". Many of their results have been meticulously studied experimentally by Fernandez-Lima et al[25-27]. In particular, they have shown experimentally that Oversampling Selective Accumulation (*OSA-TIMS*) provides higher signal to noise ratio[26,28]. Later on, Bleiholder did a comprehensive study of the trajectory of an ion (or a packet of ions) from a Langevin perspective using non-uniform electric fields in non-stationary gases[29]. The 1D Nernst-Planck balance equation for a distribution of ions of has been previously fully solved by our group showing the diffusion-correction properties of such instruments[17]. Of most significance is the fact that an initial broad distribution can be compressed axially as it travels through the system.

In this manuscript, the analytical solution of the 2D axi-symmetrical Nernst-Planck equation is provided for the first time when a linearly increasing electric field opposes a gas flow that carries the ions. The 2D axi-symmetrical solution allows the effect of a residual radial electric field -due to the solenoidal aspect of the field- to be considered together with the Axial diffusion constraint. The solution is studied for two different flows; constant $\vec{v}_{gas}$ and fully developed parabolic profile. The effect of the residual electric field has importance consequences for the stability of ions when using RF at low pressures. In fact, it precludes the possibility of using *TIMS* as an "RF-only" system for all ions. This is studied through a modified Mathieu's equation and its stability region[30]. Finally, effective resolutions of the *TIMS* instrument are provided. Given the appropriate stability conditions and electric fields, it is expected that mobility differences of less than 0.1% (equivalent resolutions larger than 1000) could be resolved at low pressures with RF and a plateau region in tubes of modest distances.

RESULTS AND DISCUSSION

Analysis of the ion motion in flows subject to opposing linearly increasing fields.

There have been multiple studies of the equations of ion motion prior to the study accomplished here. Among different studies, the most prevalent one is that of Moseley's dissertation[31], also studied by McDaniel[3], which deals with the ion motion equation and instrument resolution of a conventional drift tube. Moseley shows that a general solution of the Nernst-Planck equation for constant electric fields and no gas flow can be obtained in terms of a power series expansion. A slightly different approach for non-constant electric fields will be followed in this manuscript.

Consider a population of ions $n(z,r,t)$ of a single species created at one end of a cylindrically symmetric drift space with gas of a uniform number density N. This population is subject to a constant flow velocity in the positive z direction $\vec{v}_{gas}$ while a linearly increasing electric field E opposes the movement. Assuming that E/N is small, the Nernst-Planck equation is given by:

$$\frac{\partial n(z,r,t)}{\partial t} - \nabla \cdot \left(\overline{\overline{D}} \cdot \nabla n(z,r,t) - \left(\vec{v}_{gas} - K\vec{E}\right) n(z,r,t)\right) = 0 \quad (2a)$$

$$n(\pm\infty, \pm\infty, t) = 0\,; \;\; n(z,r,0) = f(z,r), \quad (2b,c)$$

where $f(z,r)$ corresponds to a normal distribution or a point source (See Supporting info). Here $\overline{\overline{D}}$ is the isotropic diffusion tensor. Neglecting the existence of free charge leads to a second equation (equivalent to Laplace's eq. for the potential):

$$\nabla \cdot \vec{E} = \frac{dE_z}{dz} + \frac{1}{r}\frac{drE_r}{dr} = 0 \quad (3)$$

Provided that the field in the axial direction is given by $\vec{E}_z = -Az\vec{k}$, with A constant, the solenoidal aspect of the

field (solving eq. (3)) yields the solution to the radial counterpart:

$$\vec{E}_r = \frac{Ar}{2}\vec{u}_r, \quad (4)$$

where $\vec{u}_r$ is a unit vector in the radial direction. Note that this radial component pushes the ions towards the walls. It is expected therefore that ions will tend to steer more towards the walls than in regular drift tubes. This will have implications in non-constant velocity profiles and RF containment, addressed below. *TIMS* literature uses the scan rate parameter, β, to describe the change in the slope of the electric field so that ions can be eluted. β can be related to

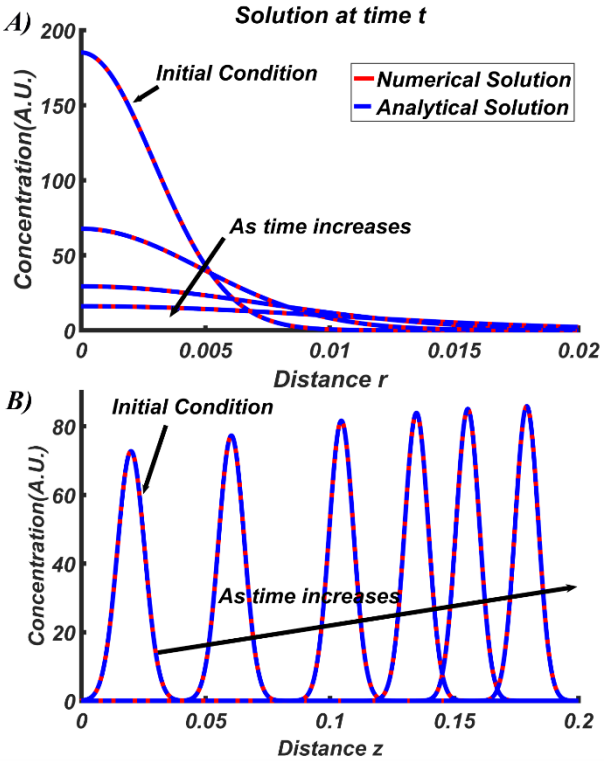

Figure 2. Comparison of numerical (using eqs. (S5-S6)) and analytical solutions (from eqs. (6-7)) for A) Radial and B) Axial directions. If a broad distribution is chosen initially in the axial direction, it is not only constrained but narrows as time passes.

the initial slope of the field A if the length of the ramp region L and the electric field in the plateau, E_e, are known: $\beta = (AL - E_e)/t$.

Eqs. (2a-c) and (3-4) form a set of partial differential equations (PDE) for which the analytical solution is desired. It is important to note that, although a 2D axi-symmetric solution is sought, an effect of angular diffusion exists. However, as long as the distribution is initially centered, the solution is invariant in the angular coordinate. Assuming no correlation between radial and axial directions, the balance population can be written as:

$$n(z,r,t) = n_z(z,t)n_r(r,t). \quad (5)$$

Being careful to account for the physical effects, a unique solution can be obtained when the initial condition is either a point source or a radially centered gaussian distribution (see Supporting info):

$$n(z,r,t) = \frac{n_s}{(2\pi)^{3/2}\sqrt{\sigma_z^2\sigma_r^2}} e^{-\frac{(z-\bar{z})^2}{2\sigma_z^2}} e^{-\frac{r^2}{2\sigma_r^2}}, \quad (6)$$

with:

$$\sigma_z^2 = \frac{2D_L}{v_{gas}}\left(\bar{z} - c_{z\sigma}\frac{KA}{2v_{gas}}\bar{z}^2\right) = \frac{D_L}{KA}(1 - c_{z\sigma}e^{-2KAt}) = \frac{kT}{qA}(1 - c_{z\sigma}e^{-2KAt}); \quad (7a)$$

$$\sigma_r^2 = \frac{2D_r}{KA}(c_{r\sigma}e^{KAt} - 1); \text{ and} \quad (7b)$$

$$\bar{z} = \frac{v_{gas}}{KA}(1 - c_{zz}e^{-KAt}). \quad (7c)$$

Here, n_s the total ion count and $c_{z\sigma} < 1$, $c_{r\sigma} > 1$, and $c_{zz} < 1$ are constants that depend on the initial condition. That eq. (6) is the solution to eqs. (2a-c) can be easily proven by inserting the solution into the equation. In Figures 2A and 2B, numerical solutions of eq. (5) with random initial conditions are superimposed on the analytical solution confirming the validity of the solution in radial and axial directions respectively. In Figure 2B, the initial standard deviation in the axial direction is purposefully chosen to be wide. As the distribution evolves, the standard deviation is reduced, proving axial confinement. The full solution for the 2D axi-symmetric problem is shown in Figure 3A at 3 different times. Given a point source as an initial condition, the distribution extends more radially than it does axially creating an oblong shape. Although the radial coordinate is represented here in a y-axis, the distribution would evolve in a radial fashion. The solution for several mobility diameters (sphere-equivalent diameter for a given mobility) is shown in Figure 3B. The ability to separate ions at a constant slope value A and constant v_{gas} is quite remarkable even with very large mobility differences thanks to the diffusion confinement in the axial direction as explored below.

Axial diffusion confinement.

It was recently shown that Axial diffusion can be regulated using two opposite controlled forces[17]. In fact, an asymptotic value for the standard deviation of a distribution of ions in the axial direction as time goes to infinity can be obtained using eq. (7a) as:

$$\sigma_{z_{t\to\infty}}^2 = \sigma_{z_{asym}}^2 = D_L/KA = kT/qA \quad (8)$$

Note that eq. (8) is fairly identical to that of the asymptotic study of Michelmann et al. (Eq. 17.15 of Supporting info) confirming the validity of eq. (6). To reach the asymptotic standard deviation, the mean value of the ion in the axial direction must also reach an asymptotic condition (from eq. (7c)) given by:

$$\bar{z}_{t\to\infty} = \bar{z}_{asym} = v_{gas}/KA. \quad (9)$$

The asymptotic standard deviation, eq. (8), is independent of diffusion or mobility allowing this type of confinement to be used for large and small ions. It is also in inverse proportion to field slope A and the charge q. It can be extrapolated that the only limiting factor to get any desired separation -i.e. effective resolutions in the order of thousands- is the limitation in the maximum slope A that can be applied. A combination of four factors determine the maximum slope: 1) the gas electrical breakdown, 2) the gas flow velocity v_{gas}, 3) the total length of the drift chamber and 4) the mobility/mobilities K one is interested in separating. While the first factor is quite obvious, the other three have

to do with the fact that not all mobilities necessarily reach asymptotic conditions for a given set of conditions. For example, very low mobilities would require either very high slopes or very small velocities to be trapped. Simultaneously, for any real separation to occur, v_{gas} has to be large enough so that the distance between the mean values of two particular mobilities $\bar{z}_1$ and $\bar{z}_2$ is greater than the full width at half maximum (FWHM) of either peak. This definition of separation best represents the instrument performance as opposed to the more widely used resolution (see below). It is however true that an asymptotic effective resolution can still be obtained from eqs. (8-9).

It is important to note that the above asymptotic solution can be reached regardless of the initial condition. This is a substantial advantage over other systems as unusually broad distributions can be sampled into the system and still be corrected axially if sufficient time is given. This effect, mostly unexplored, could be used to accumulate ions for long periods and subject to lower space charge.

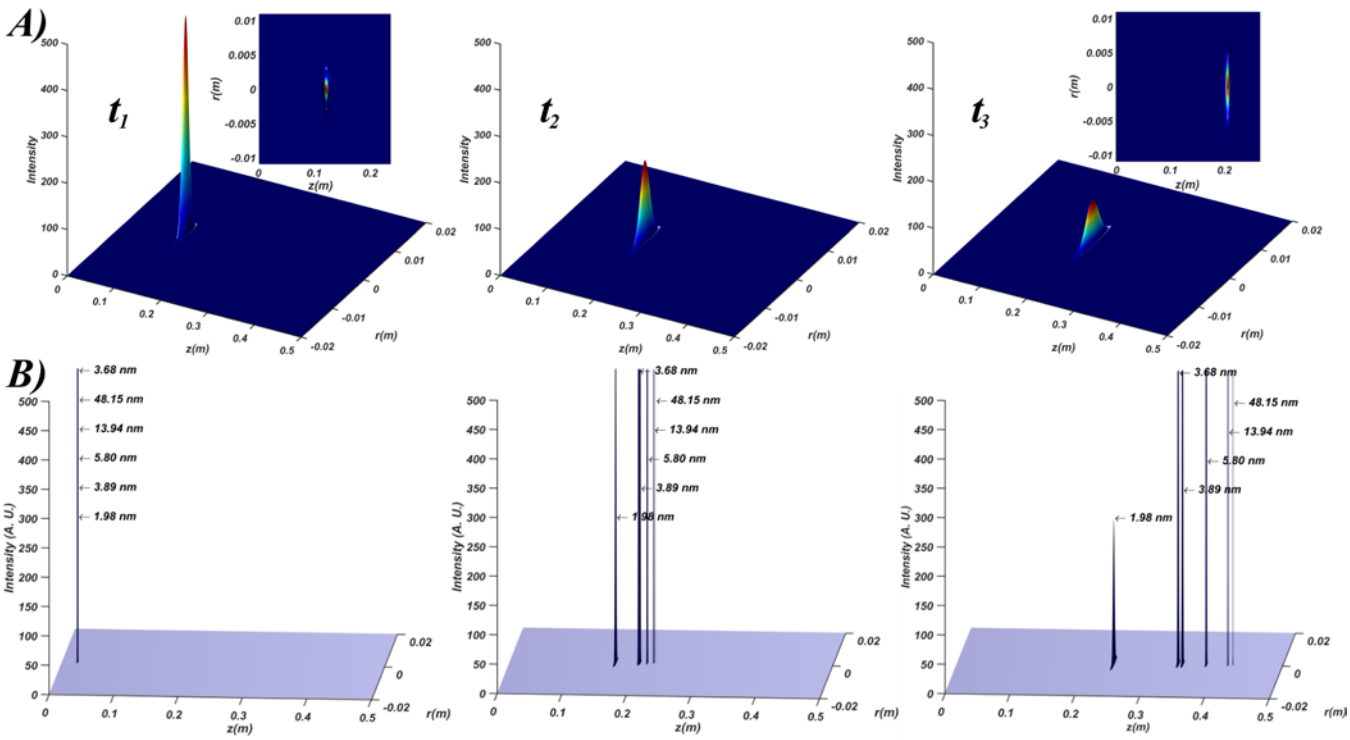

Figure 3 A) Evolution of a three-dimensional mobility distribution as it progresses through the ramp region of the instrument at three different instants in time (no RF). As the distribution progresses, ions freely migrate radially but are contained in the axial direction (see insets). The axial distribution width has been purposefully enhanced by a factor of 10. B) Evolution of packets of ions of different mobilities (singly charged spheres of given diameters) as they are being separated in the ramp region. More mobile ions diffuse more radially. However, they are all contained axially.

Non-constant velocity profiles and tail forming.

Previous Nernst-Planck equation (eqs. (2a-c)) has been solved assuming that v_{gas} is a constant in the axial direction.

However, this is not accurate. In general, in a constant section tube, a flow will eventually evolve into a parabolic profile. For a tube with a radius r_0, the flow velocity for a fully developed parabolic profile with maximum velocity v_{max} is:

$$v_{gas} = v_{max}(1 - r^2/r_0^2). \quad (10)$$

Parabolic profiles have been shown to be accurate for *TIMS* geometries using CFD[23]. Under such circumstances, eq. (2) becomes coupled and the ion distribution solution becomes convoluted (eq. (5) is not valid). An approximation to the analytical solution, however can be explored and compared to a numerical solution, obtained using SIMION 8.1. Figure 4A shows the result when packets of ions of up to 6 different mobilities are stopped inside the tube for a constant slope A, atmospheric pressure and no RF. The simulation was specifically adapted to represent an ideal situation of a tube with linearly increasing field. Ions start centered, migrate through the tube, and are eventually stopped at the asymptotic mean value (eq. (9)). At this point, they drift-diffuse radially. In contrast to the perpendicular migration perceived with constant gas flow, ions are now pulled back trying to match gas and drift velocity. As the ions are pulled farther away from the center, the radial electric field becomes more prominent than either drift or gas velocity and ions are pushed towards the electrodes. It is encouraging to observe the little axial diffusion present even though multiple ions where used to form the trajectories of each curve.

An approximation to an analytical solution can be obtained when the variation of the velocity is assumed to be small ($dv_{gas}/dr \sim 0$). Under such circumstances the mean of the distribution is given by:

$$\bar{z} = \frac{v_{max}(1-r^2/r_0^2)}{KA}(1 - c_{zz}e^{-KAt}). \quad (11)$$

The analytical approximation states that, as an ion diffuses radially, it has enough time to accommodate to the

change in the velocity of the gas by reducing its drift velocity. This, however, would not be physically true as far away from the center and towards the electrodes, the radial drift due to the residual radial electric field would be too large for the ion to equilibrate axial drift and gas velocity. Indeed, when comparing the mean values of the analytical approximation to the SIMION solution, as shown in Figure 4B, they agree remarkably well close to the center but deviate farther away from the center. This is more prominent for higher mobility ions as diffusion occurs more quickly.

The full analytical solution should be of the type:

$$\bar{z} = \frac{v_{max}(1-2r^2/r_0^2 e^{-\ r^2/r_0^2})}{KA}(1 - c_{zz}e^{-KAt}) \qquad (12)$$

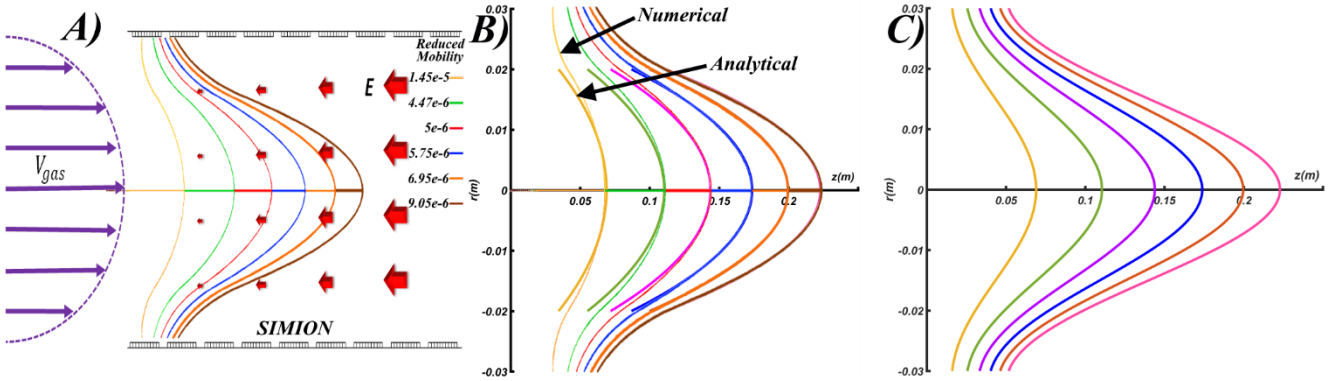

Figure 4. A) SIMION 8.1 trajectory results of packages of singly charged spherical ions of 6 different mobilities being axially trapped in a tube with a parabolic velocity profile and no RF. Ions start centered, migrate through the tube and stop when $\Lambda = 1$. At that point they drift-diffuse radially. B) Superposition of analytical approximation eq. (11) when $(dv_{gas})/dr \sim 0$ and SIMION 8.1 trajectories. C) Analytical approximation using eq. (12).

parabolic and constant velocity profiles when ions are collected a distance L from the particle insertion point. Figure 5A shows the effect of the tails when multiple mobilities are present. While the tail might not be significant for a single mobility ion, it can become a large problem when multiple mobilities are present. In contrast, Figure 5B shows the ions under constant gas velocity and where all ions can be easily differentiated. Although the re-percussions of the tail will be of paramount importance when no RF is present, they may also become important with RF and high mobility ions.

Aside from RF, there are ways to avoid or attenuate the problem. One possibility is to insert the ions centered in the tube. Since the radial electric field is proportional to r, it is extremely weak in the center and the radial migration of the ions can be hampered. Another way is to taper the tube so that a plug flow is formed leading to a more constant velocity in the center. A last resort is to collect the ions only at the center with the corresponding signal loss.

The results from eq. (12) are shown in Figure 4C. Note that eq. (12) is an asymptotic solution. No attempt to find the full analytical solution is made in the present manuscript.

The importance of the parabolic velocity profile should not be underestimated, especially at atmospheric pressure as it could seriously impair the resolution of the instrument if left unchecked. If ions are allowed to migrate through the ramp ($\Lambda < 1$) and collected by a detector, long tails might appear due to the half-moon shaped distributions created. Figure 5 shows a comparison between

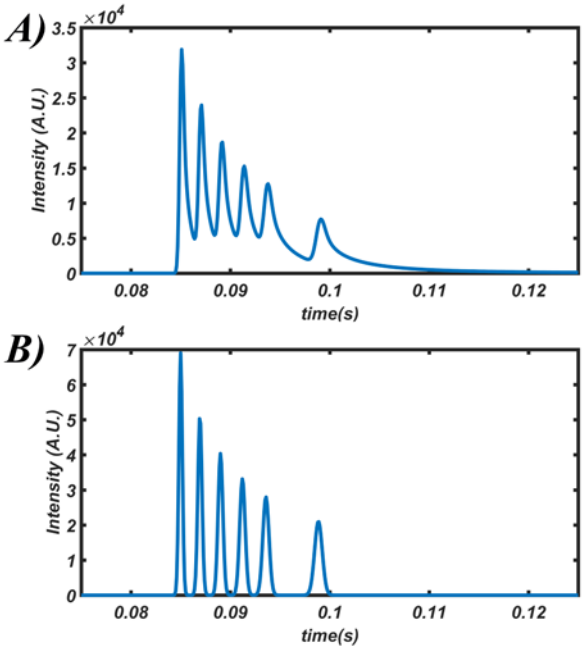

Figure 5. Intensity as a function of time for ions collected a distance L downstream in an *IDT* with no RF for A) parabolic velocity profile and B) constant velocity profile. Note the effect of the tails created in A).

Radial Losses and RF confinement at low pressures.

A relevant issue appearing when using a linearly increasing electric field in the axial direction is the appearance of a residual electric field to comply with the

divergence (eqs. (3-4)). This radial field pushes the ions outwards augmenting the effect of regular radial diffusion. This becomes quite problematic, especially at high pressures where RF cannot be used. At such pressures, the only possibility to avoid large diffusion losses is to have the ions as centered as possible initially while keeping them in the tube for the shortest possible time. This requires the separation ratio Λ to be small, hampering the overall resolution that the *IDT* instrument can achieve.

At low pressures, RF can and should be used to contain the ions. However, the existence of the residual field (eq. (4)) complicates the use of RF as an all-ion guide. To study the effect of this field on the stability of the ions, an ideal RF potential for 4 hyperbolic rods may be superimposed on the axial potential:

$$\Phi = \frac{\Phi_0}{2r_0^2}(x^2 - y^2) \;\; ; \;\; \Phi_0 = U + Vcos(wt + \theta_0), \qquad (13)$$

Here, w is the RF driving frequency, θ_0 the initial phase, and U and V are the DC and AC potentials applied respectively. In general, for RF guide-only mode, U should equal to 0. With $U = 0$, and considering the effect of drag, the radial equations of motion ($\vec{F} = q\vec{E} - \vec{F}_{drag} = M\vec{a}$) in Cartesian coordinates are:

$$M\frac{d^2x}{dt^2} - \frac{qx}{r_0^2}\left(\frac{A}{2} + Vcos(wt + \theta_0)\right) + \frac{q}{K}\frac{dx}{dt} = 0; \qquad (14a)$$

$$M\frac{d^2y}{dt^2} - \frac{qy}{r_0^2}\left(\frac{A}{2} - Vcos(wt + \theta_0)\right) + \frac{q}{K}\frac{dy}{dt} = 0. \qquad (14b)$$

Here, the third term corresponds to the drag, proportional to the velocity, and is given, e.g. in eq. (14a), in terms of ion mobility as $\frac{q}{K}\frac{dx}{dt}$. The electric field (second term) is a composition of the field provided by Φ and that provided by eq. (4) (See Supporting info). Due to the residual radial electric field, the equations of motion carry a DC-equivalent potential that cannot be avoided, as if U had been chosen to be $-A/2$. $A/2$, unlike U, cannot be chosen to be 0 and will play a key role in the stability of the ions. Note that this DC potential is also different from the one applied in quadrupoles[32] as it has the same sign on both eqs. (14a-b). With a change of variables, eqs. (14a-b) become the Mathieu eqs.:

$$\frac{d^2u}{d\xi^2} - \left(a_u \pm 2q_u cos(2\xi)\right)u + \frac{2q}{wmK}\frac{du}{d\xi} = 0\,; \qquad (14c)$$

$$\xi = \frac{wt}{2} \;; a_u = \frac{2qA}{w^2r_0^2m} \;; q_u = \frac{2qV}{w^2r_0^2m}, \qquad (14d\text{-}f)$$

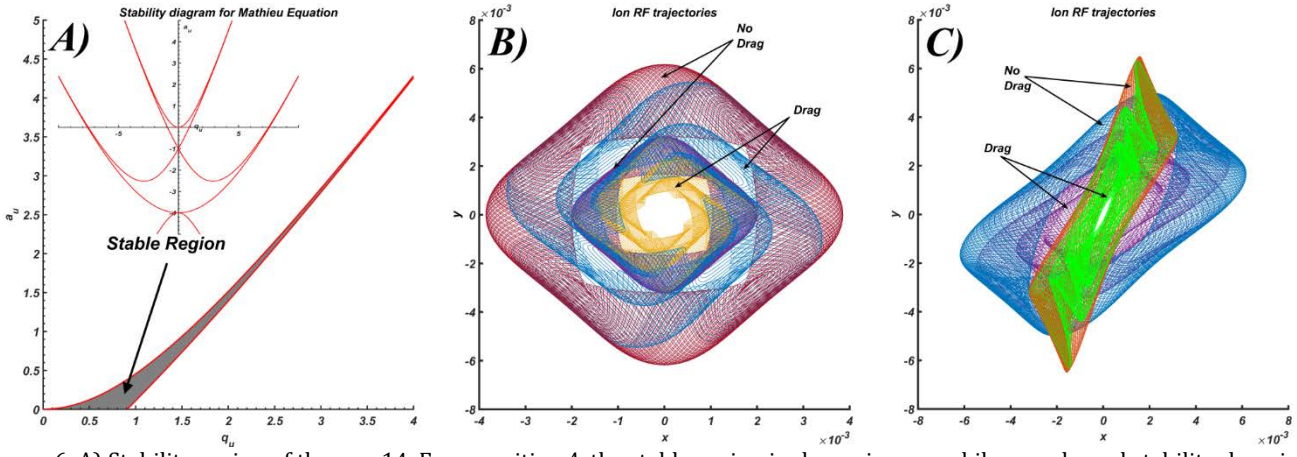

Figure 6. A) Stability region of the eqs. 14. For a positive A, the stable region is shown in gray while an enlarged stability domain is shown in the inset. B) RF confinement ion trajectories with and without drag for initial velocities parallel to one of the axis and non-centered initial positions. C) RF confinement ion trajectories with and without drag for initial velocities at 45 degrees.

where u represents either x or y. Figure 6A shows the stability domain for eqs. (14c) when drag is considered negligible, e.g. vacuum conditions. Drag at low pressures has been shown to have little influence on stability, slightly enlarging the stability region[33,34]. Due to the requirement of always having an equivalent non-zero DC potential, not all masses are stable at all frequencies, and care must be had to not lose ions in the process. For example, if the slope A was reduced at some point (smaller a_u), it could potentially lead to some ions becoming unstable. To avoid this, q_u would have to be simultaneously reduced.

The motion of ions on stable trajectories is shown in Figures 6B-C for different initial conditions of position and velocity of the ions. When drag is not considered, the trajectories are confined to a region that depends strongly on the initial conditions and phase. Figure 6B shows trajectories with initial velocities parallel to one of the axes for θ_0 at 0 and 180 degrees. Figure 6C shows initial velocities at 45 degrees. When drag is considered, stable trajectories tend towards the center as shown in Figures 6B-C. Random walk diffusion is not considered and could potentially affect the ion stability.

Effective resolutions using RF confinements.

Asymptotic resolution of the ramp region.

In a previous manuscript[17], it was described how resolution, in its common definition used for drift tube ion mobility, $\bar{z}/\Delta z$, was an ill-conditioned parameter for *IDT*. As an example, one can look at the case of an *IDT* with no field present where ions of different mobilities would reach the detector simultaneously. Despite the very high resolution in terms of $\bar{z}/\Delta z$, there would be no separation. A better alternative is to use the resolving power employed in chromatography for two peaks; given by the ratio of the distance between two peak centers, $\Delta\bar{z}$, and the average full width at half maximum, $\overline{FWHM}$, minus 1; $R_p = \frac{\Delta\bar{z}}{\overline{FWHM}} - 1$. From its definition, one should expect two peaks to be resolved if $R_p > 0$. R_p can be used to obtain effective resolutions. For instance, for the *TIMS* instrument, an effective asymptotic resolution for the ramp (trapped) region can be obtained

when the separation ratio Λ reaches 1 (See Supporting info):

$$R_{\Lambda\to 1} = \frac{\bar{z}_{asym}}{\overline{FWHM}_{asym}} \quad (15)$$

Here, for a resolution of 100, the instrument will be able to resolve two mobilities that differ 1%. Given eqs. (8-9) and assuming that, for two very close mobilities, $\overline{FWHM}_{asym} \sim 2\sqrt{2\ln(2)\,\sigma^2_{\bar{z}asym}}$, the asymptotic resolution for a ramp of length L yields (see Supporting info):

$$R_{\Lambda\to 1} = \sqrt{\frac{v_{gas}^2}{8\ln(2)KAD}} = \sqrt{\frac{qv_{gas}L}{8\ln(2)k_bTK}} = \sqrt{\frac{qAL^2}{8\ln(2)k_bT}} = \sqrt{\frac{qLE_{\bar{z}=L}}{8\ln(2)k_bT}}. \quad (16a\text{-}d)$$

It is assumed that the separation ratio Λ reaches one at the end of the ramp so that $\bar{z}_{asym} = L$, being $E_{\bar{z}=L} = AL$ the corresponding electric field. Despite the similarity of eq. (16d) to the *DTIMS* resolution, there are marked differences between the two. The most important one is that the electric field is not constant like in a DTIMS. The field required to reach $\Lambda = 1$ at the end of the tube will therefore depend on the mobility and the velocity of the gas. Moreover, given the quadratic nature of the voltage employed, one has to be careful to avoid breakdown scenarios. In order to explore these dependencies, it is better to use the second expression for the resolution, which has a direct dependence on K, v_{gas}, L; eq. (16b). Figure 7A shows the dependence of the resolution on reduced mobility, K_0, for a L=50cm ramp with different gas velocities, v_{gas}, ranging from 50 to 200m/s at two different pressures and a temperature of 300K. Resolution shows an inverse square root dependence with mobility and a marked increase at higher pressures. At a commonly used gas flow of 150m/s[23], resolutions of ~200 can be reached for reduced mobilities of $K_0 = 0.5cm^2/Vs$ ($CCS \sim 210A^2$). The voltage required however to trap this mobility would be around 4.0kV at 0.5m ($V = v_{gas}L/2K$). For different reduced mobilities $K_0 = 0.3 - 1.1\ cm^2/Vs$, the change in resolution with gas velocity for L=50cm and pressure of 2.5 torr is given in Figure 7B. The resolution of the ramp region has been somewhat ignored in previous theoretical assessments of the *TIMS* instrument due to the difficulty in solving eq. (2a-c). As shown here, it could be of strong consequence if treated correctly and especially if coupled with the plateau region of the *TIMS* described below.

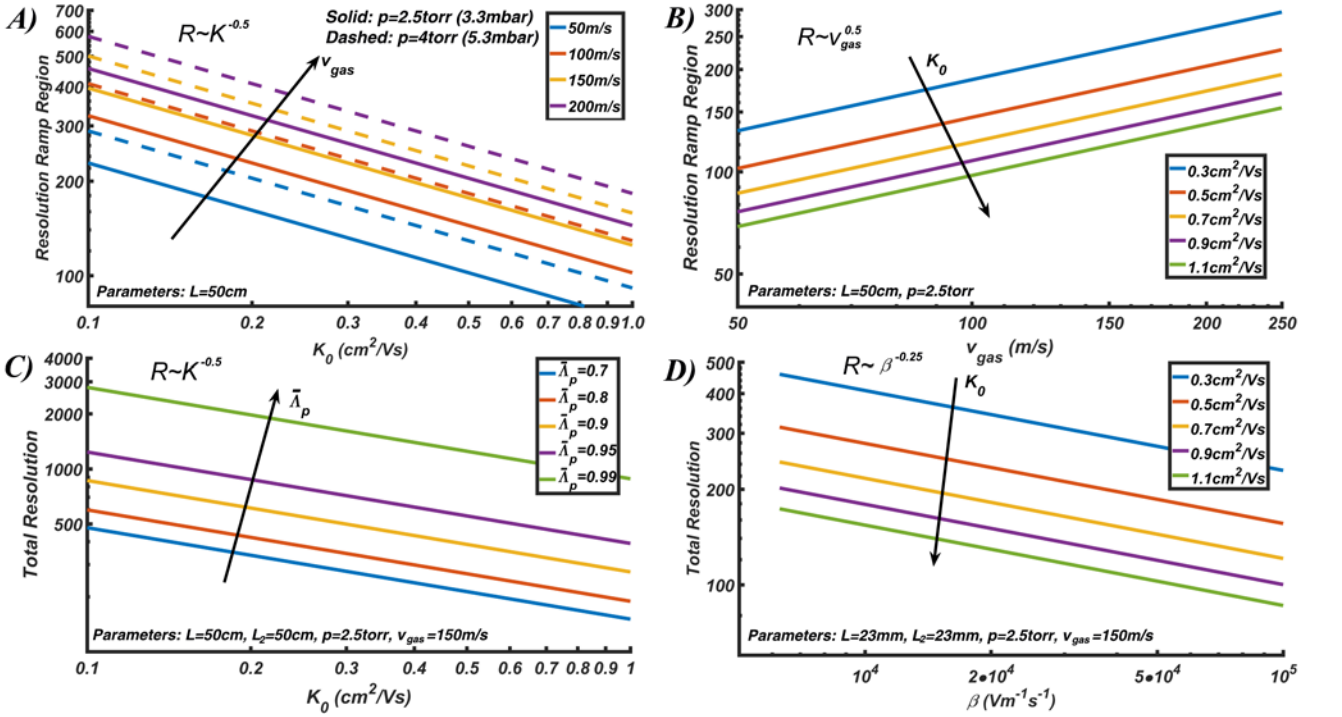

Figure 7. Asymptotic resolutions of the ramp and plateau regions. A) Ramp Resolution $R_{\Lambda\to 1}$ as a function of reduced mobility K_0 for different gas velocities. B) $R_{\Lambda\to 1}$ as a function of v_{gas} for different reduced mobilities K_0. C) R_{total} as a function of reduced mobility K_0 for different average separation ratios $\bar{\Lambda}_p$. D) R_{total} as a function of the scan rate β for different reduced mobilities.

Resolution in the plateau region.

To take advantage of the ramp separation and asymptotic resolution, a way to elute the ions must be included to collect them in a detector or be transferred to a Mass Spectrometer. The most reasonable way to elute the ions, is to reduce the slope A of the electric field a sufficient amount so that ions drift outside of the trapping region. Once lowered, the ions start moving through the plateau region. This plateau region follows a separation procedure similar to that of the drift tube but where the velocity of the gas carries the ion forward while the position-independent electric field, E_e, opposes the flow. Using the definition of Resolving power (See Supporting info), one can calculate the effective resolution. The resolution for a plateau of length L_2 is given by:

$$R_{plateau} = \sqrt{\frac{qL_2\Lambda_pE_e}{(1-\Lambda_p)16ln2k_bT}} = \sqrt{\frac{qL_{2,eff}E_e}{16ln2k_bT}} \quad (17)$$

Here, the separation ratio in the plateau, $\Lambda_p = KE_e/v_{gas}$, must be lower than one to allow ions to move through the plateau with velocity $\vec{v}_{ion} = \vec{v}_{gas}(1-\Lambda_p)$. The closer Λ_p

is to 1, the higher the resolution. One can introduce an effective length, $L_{2,eff} = L_2\Lambda_p/(1-\Lambda_p)$, to compare the plateau region to a *DTIMS*. If the separation ratio is lowered to $\Lambda_p = 0.8$, then the effective length of the plateau region would be 4 times its total length $(0.8/(1-0.8))$. One can drastically increase the effective length to boost the resolution, e.g. by almost 10-fold at $\Lambda_p = 0.99$. The increase in resolution, however, comes at a cost. Since the elution is time-based and there is no diffusion control in the plateau, peaks will tend to broaden as they become separated, greatly decreasing the peak maximums. A compromise must then be made between peak max intensity and resolution. Eq. (17) differs from the resolution previously derived for the *TIMS*[24]. Aside from other simplifications, the previous resolution assumed that the eluting electric field changes over time at a given rate. Resolution in eq. (17) can consider changes in the electric field by assuming that the separation ratio changes with time, $\Lambda_p = \Lambda_p(t)$. In fact, for linear changes in the slope of the field, an average value of the separation ratio $\bar{\Lambda}_p$ can be used as a substitute in eq. (17). $\bar{\Lambda}_p$ can then be related to the scan rate β by (See Supporting info):

$$\bar{\Lambda}_p = 1 - \sqrt{\frac{L_2 K \beta}{2 v_{gas}^2}} \qquad (18)$$

Combined resolution for TIMS.

The overall resolution is a complicated convolution of both regions, ramp and plateau and is given by (See Supporting info):

$$R_{total} = \frac{(L_{2,eff}+L)\sqrt{E_e q}}{\sqrt{8 ln2 k_b T (L\bar{\Lambda}_p + 2L_{2,eff})}} \qquad (19)$$

When $L_{2,eff} \gg L$, i.e., the effective plateau length is much larger than the length of the ramp region, eq. (19) reduces to previous reported resolutions except for a factor of $\bar{\Lambda}_p$, due, perhaps, to different simplifications[24]. Figure 7C shows the combined resolution for a plateau length of L_2=50cm as a function of the change in $\bar{\Lambda}_p$ from 0.7 to 0.99 for different reduced mobilities K_0. While resolutions are extremely high for very high plateau separation ratios, it will involve losing max peak intensity, and care must be taken. It is easy to observe that the length of the plateau L_2 is not as important as the separation ratio used. In principle one could have a very small physical length and still achieve high separation if a large separation ratio $\bar{\Lambda}_p$ would be employed. In fact, this can be observed when one tries to obtain the resolution of the *TIMS* instrument with only 46mm in length. Figure 7D shows such resolution as a function of the scan rate, β, using eq. (18) and assuming that the scan rate is linear with time, as is the case in *TIMS*. The slower the scan rate, the higher the resolution (higher average separation ratios). The proportionality $R_{total} \sim \beta^{-0.25}$ in Figure 7D is not exact as derived from the equations. Under all scenarios presented, it is considered that the ions inside the ramp have reached its asymptotic condition. This might not be the case if the scan rate is too fast.

The resolutions obtained here should be considered an upper bound as they neglect the effects of parabolic velocity profiles. However, R~400 have already been obtained experimentally in *TIMS* revealing the instrument possibilities[35]. The greatest benefit of these systems, not possible in a *DTIMS*, is that, regardless of the initial width of the package of ions, well-defined asymptotic distributions are guaranteed at the beginning of the plateau region thanks to the confinement in the ramp.

CONCLUSIONS

The ability of instruments with linearly increasing fields to provide high resolutions and compact distributions due to their diffusion-confining ability has been explored. A solution to the 2D Nernst-Planck equation is provided for the first time. The way axial diffusion confining is generated, i.e. equilibrium between the electric field and gas flow, however, leads to important issues that may hamper resolution and/or sensitivity. The main two issues, covered in this manuscript, are the formation of parabolic velocity profiles and the existence of residual radial field components. Both issues can be avoided at low pressures with the help of RF radial confinement. A regular RF only ion guide, however, would not be sufficient to contain all ions and a frequency range must be employed to avoid ion loss. Atmospheric pressure precludes the use of RF so reducing the effects of the velocity profiles and residual fields is the only possibility. The fact that resolution is indirectly proportional to the square root of the mobility makes *IDT* a perfect candidate for larger species (~100nm), if the issues are resolved/ contained.

In conclusion, *TIMS* and *IDT* systems have excellent separation capabilities with resolutions that rival the best gas phase separation systems. The new insights in this manuscript open a new path to further develop these instruments with great potential in the fields of Analytical Chemistry and Aerosol Science.

ASSOCIATED CONTENT

Supporting Information

The Supporting Information is available free of charge on the ACS Publications website.

Mathematical description of resolving powers, solution to the 2D axi-symmetric Nernst-Planck equation for field and gas velocity, explanation of Laplace and RF Ion Motion (eqs.(4) and (14)).

AUTHOR INFORMATION

Corresponding Author

*E-mail: clarriba@iupui.edu

ACKNOWLEDGMENT

This manuscript was supported by Kanomax Japan Inc. and Kanomax-FMT USA through grant award KC IP ID 00487260.

REFERENCES

(1) Ounis, H.; Ahmadi, G.; Mclaughlin, J. B. *J Colloid Interf Sci* **1991**, *143*, 266-277.
(2) Davies, C. N. *Proceedings of the Physical Society* **1945**, *57*, 259.
(3) Mason, E. A.; McDaniel, E. W. *Transport properties of ions in gases*; John Wiley & Sons.: New York, 1988.
(4) Larriba, C.; Hogan, C. J. *J Phys Chem A* **2013**, *117*, 3887-3901.
(5) Albritton, D. L.; Miller, T.; Martin, D.; McDaniel, E. *Physical Review* **1968**, *171*, 94.
(6) Knutson, E.; Whitby, K. *J Aerosol Sci* **1975**, *6*, 443-451.

(7) Smith, D. P.; Knapman, T. W.; Campuzano, I.; Malham, R. W.; Berryman, J. T.; Radford, S. E.; Ashcroft, A. E. *European journal of mass spectrometry* **2008**, *15*, 113-130.
(8) Kolakowski, B. M.; Mester, Z. *Analyst* **2007**, *132*, 842-864.
(9) Valentine, S. J.; Stokes, S. T.; Kurulugama, R. T.; Nachtigall, F. M.; Clemmer, D. E. *J Am Soc Mass Spectr* **2009**, *20*, 738-750.
(10) Krylov, E.; Nazarov, E.; Miller, R. *Int J Mass Spectrom* **2007**, *266*, 76-85.
(11) Flagan, R. C. *Aerosol Sci Tech* **2004**, *38*, 890-899.
(12) Kulkarni, P.; Wang, J. *J Aerosol Sci* **2006**, *37*, 1326-1339.
(13) Webb, I. K.; Garimella, S. V. B.; Tolmachev, A. V.; Chen, T. C.; Zhang, X. Y.; Cox, J. T.; Norheim, R. V.; Prost, S. A.; LaMarche, B.; Anderson, G. A.; Ibrahim, Y. M.; Smith, R. D. *Analytical Chemistry* **2014**, *86*, 9632-9637.
(14) Arffman, A.; Juuti, P.; Harra, J.; Keskinen, J. *Aerosol Sci Tech* **2017**, 1-9.
(15) Fernandez-Lima, F.; Kaplan, D. A.; Suetering, J.; Park, M. A. *International Journal for Ion Mobility Spectrometry* **2011**, *14*, 93-98.
(16) Ridgeway, M. E.; Lubeck, M.; Jordens, J.; Mann, M.; Park, M. A. *Int J Mass Spectrom* **2018**, *425*, 22-35.
(17) Nahin, M.; Oberreit, D.; Fukushima, N.; Larriba-Andaluz, C. *Sci Rep-Uk* **2017**, *7*.
(18) Allen, S. J.; Bush, M. F. *J Am Soc Mass Spectr* **2016**, *27*, 2054-2063.
(19) Sutherland, W. *The London, Edinburgh, and Dublin Philosophical Magazine and Journal of Science* **1905**, *9*, 781-785.
(20) Deng, L. L.; Ibrahim, Y. M.; Baker, E. S.; Aly, N. A.; Hamid, A. M.; Zhang, X.; Zheng, X. Y.; Garimella, S. V. B.; Webb, I. K.; Prost, S. A.; Sandoval, J. A.; Norheim, R. V.; Anderson, G. A.; Tolmachev, A. V.; Smith, R. D. *Chemistryselect* **2016**, *1*, 2396-2399.
(21) Zeleny, J. *The London, Edinburgh, and Dublin Philosophical Magazine and Journal of Science* **1898**, *46*, 120-154.
(22) Huang, Z.; Ivory, C. F. *Analytical Chemistry* **1999**, *71*, 1628-1632.
(23) Silveira, J. A.; Michelmann, K.; Ridgeway, M. E.; Park, M. A. *J Am Soc Mass Spectr* **2016**, *27*, 585-595.
(24) Michelmann, K.; Silveira, J. A.; Ridgeway, M. E.; Park, M. A. *J Am Soc Mass Spectr* **2015**, *26*, 14-24.
(25) Tose, L. V.; Benigni, P.; Leyva, D.; Sundberg, A.; Ramirez, C. E.; Ridgeway, M. E.; Park, M. A.; Romao, W.; Jaffe, R.; Fernandez-Lima, F. *Rapid Commun Mass Sp* **2018**, *32*, 1287-1295.
(26) Benigni, P.; Fernandez-Lima, F. *Analytical Chemistry* **2016**, *88*, 7404-7412.
(27) Hernandez, D. R.; DeBord, J. D.; Ridgeway, M. E.; Kaplan, D. A.; Park, M. A.; Fernandez-Lima, F. *Analyst* **2014**, *139*, 1913-1921.
(28) Benigni, P.; Porter, J.; Ridgeway, M. E.; Park, M. A.; Fernandez-Lima, F. *Analytical Chemistry* **2018**, *90*, 2446-2450.
(29) Bleiholder, C. *Int J Mass Spectrom* **2016**, *399*, 1-9.
(30) Paul, W. *Rev Mod Phys* **1990**, *62*, 531-540.
(31) Moseley, J. T. *Thesis Dissertation, Georgia Tech* **1968**, Chapter V.
(32) Miller, P. E.; Denton, M. B. *J Chem Educ* **1986**, *63*, 617.
(33) Nasse, M.; Foot, C. *Eur J Phys* **2001**, *22*, 563-573.
(34) Viehland, L. A.; Goeringer, D. E. *J Chem Phys* **2004**, *120*, 9090-9103.
(35) Adams, K. J.; Montero, D.; Aga, D.; Fernandez-Lima, F. *International Journal for Ion Mobility Spectrometry* **2016**, *19*, 69-76.

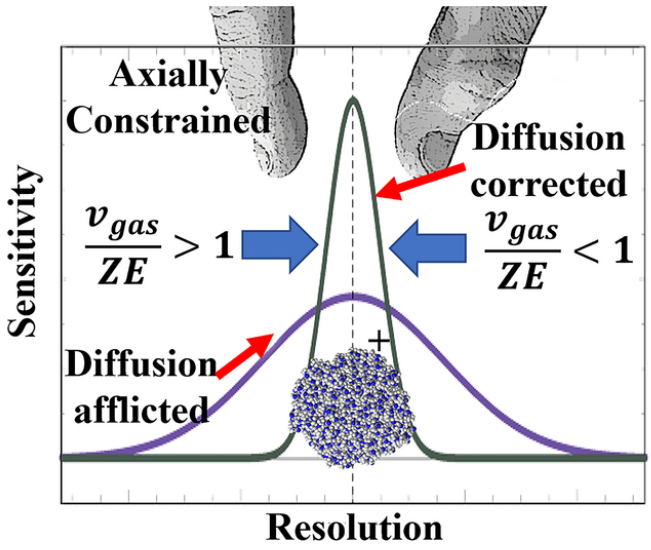

82x44mm (300 x 300 DPI)